ANNALI DI GEOFISICA, VOL. XXXVI, N. 2, May 1993

Pleistocene rotations and strain in southern Italy: the example of the Sant'Arcangelo basin

Leonardo Sagnotti and Antonio Meloni
Istituto Nazionale di Geofisica, Roma, Italia

Abstract
Results of paleomagnetic and magnetic-fabric analyses carried out on Upper Pliocene and Lower Pleistocene clayey units of the Sant'Arcangelo basin, in the southern Apennines, Italy, are shown. The reconstructed magnetic fabrics, typical of sediments at the very first stage of deformation, depend on the structural position of the sampling sites and reflect the orientation of Pleistocene maximum compressive stress in the area. The paleomagnetic data indicate that the basin underwent a counterclockwise rotation of about 22° after the deposition of the Lower Pleistocene clays. The data obtained in this study are compared with those already published for coeval deposits in southern Italy and are considered in the framework of the Pleistocene geodynamic evolution of the region.

1. Introduction

The structural setting of southern Italy is the result of complex geodynamic events which succeeded from late Tortonian up to the present (Patacca and Scandone, 1989; Patacca *et al.*, 1990). There are several different kinds of geological approaches for studying geodynamic evolution, among these the studies concerning the magnetic properties of rocks constitute a powerful method both for the investigation of the effects of strain on rocks magnetic fabric (by means of analysis of Anisotropy of Magnetic Susceptibility (AMS)) as well as for the identification of possible crustal blocks vertical-axis rotations (by means of analysis of Natural Remanent Magnetization (NRM) or, properly, paleomagnetic studies).

For southern Italy no AMS data are available in the literature for the sedimentary units of the Apennines thrust belt and most of published paleomagnetic data concerns Mesozoic units (see Incoronato and Nardi, 1989 for a review). Results generally indicate the occurrence of various amounts of counterclockwise rotation in the southern Apennines and clockwise rotation in the allochtonous Sicily. However, some studies on southern Italy Plio-Pleistocene sediments (Tauxe *et al.*, 1983; Aifa *et al.*, 1988; Scheepers *et al.*, 1991) show that the tectonics associated with the most recent phases of geodynamic evolution produced, in large amount, vertical-axis rotations even in the Pleistocene units. In this framework, this paper deals with the analyses of the magnetic properties of some Plio-Pleistocene sediments from the Sant'Arcangelo basin in the southern Apennines (Sagnotti, 1992; Sagnotti and Speranza, 1992). Obtained results contribute to the study of the vertical-axis rotations occurred in southern Italy during Pleistocene times and also to the definition of the strain pattern in the basin itself.

2. Geological setting of the Sant'Arcangelo basin

The Sant'Arcangelo basin (fig. 1) is internal to the front of the allochtonous thrust sheets of the southern Apennines chain and is structurally

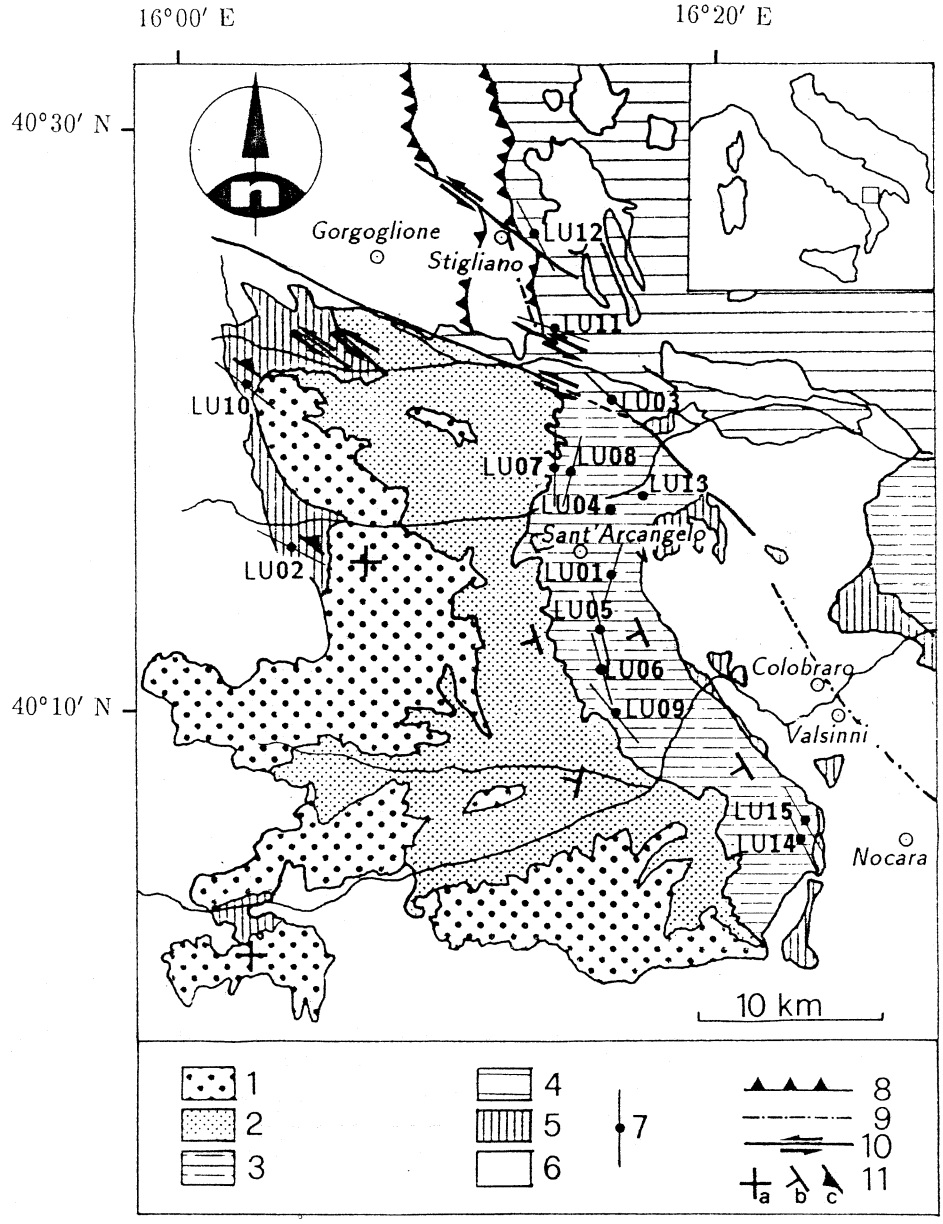

Fig. 1. Geological sketch of the Sant'Arcangelo basin area (from Hippolyte *et al.*, 1991, simplified and modified). Location of the mapped area is shown in the inset upper right. Upper Pliocene-Lower Pleistocene cycle: 1) conglomerates. 2) Sands. 3) Marly-clays. 4) Pliocene and Pleistocene. 5) Upper Pliocene. 6) Undifferentiated allochton. 7) Sampling site with axis corresponding to k_{max} maximum density. 8) Overthrusts front. 9) Anticline axis. 10) Left- lateral strike-slip fault. 11) Bedding attitude. a) Dip , 10°, b) dip (10÷30)°, c) dip $> 30°$.

interpreted as a «piggyback» basin (Hippolyte *et al.*, 1991).

The basin is filled with thick terrigenous Plio-Pleistocene sequences referred to distinct sedimentary phases (Vezzani, 1967; Caldara *et al.*, 1988). A typical regressive sequence of Upper Pliocene-Lower Pleistocene age, with a basal clayey unit passing up and westward to sands and finally to conglomerates, outcrops extensively in the basin. This sequence is weakly deformed and defines a broad NW-SE syncline with some minor folds. An older sequence, Upper Pliocene in age, outcrops only at the western and eastern edges of the basin and shows a rather complex pattern of deformation and a strong tilting with the strata dipping up to 65°. A WNW-ESE left-lateral strike-slip fault constitutes the northern border of the basin; north of this fault eastward vergent thrusts are widely developed. At the outermost thrust front Miocene flyschoids sediments override Upper Pliocene clays. Evidence of synsedimentary tectonics was recently found (Caldara *et al.*, 1988; Hippolyte *et al.*, 1991). In particular, the mesostructural analysis performed by Hippolyte *et al.* (1991) indicated the existence of a Pleistocene compressive episode with the maximum compressional stress (σ_1) oriented N70° (±13), both in and out the basin. Traces of a previous Pliocene compression, with σ_1 oriented N20°, were also recognized.

3. Sampling and measurements

Our analysis was carried out on 182 oriented cores sampled at 15 sites in the Plio-Pleistocene clayey units outcropping in the Sant'Arcangelo basin area (fig. 1). 10 sampling sites are in the eastern flank of the main syncline (in Lower Pleistocene clays (NN19 nannofossil zone; Hippolite *et al.*, 1991)), 2 are in the western edge of the basin (in Upper Pliocene clays (NN14-NN16 nannofossil zones, Hippolite *et al.*, 1991 and Globorotalia puncticulata zone, Vezzani, 1967)) and 3 are north of the basin (in Upper Pliocene clays; Lentini, 1979). Magnetic-fabric and paleomagnetic analyses were performed in the new paleomagnetic laboratory of the Istituto Nazionale di Geofisica, in L'Aquila, Italy. One standard specimen (25 mm in diameter, 22 mm high) for each core was analyzed; both Anisotropy of Magnetic Susceptibility (AMS) and Natural Remanent Magnetization (NRM) were measured; AMS measurements were performed using a KLY-2 KappaBridge; NRM measurements, at different stages of stepwise thermal demagnetization, were carried out using a JR-4 spinner magnetometer.

4. Anisotropy of Magnetic Susceptibility (AMS) data

The mean susceptibility of the analyzed specimens ranges from 1.7×10^{-3} to 1.6×10^{-4} SI units. The overall analysis of the AMS data obtained from each specimen indicates that the magnetic foliation clearly prevails on the magnetic lineation and that the anisotropy degree (P' parameter; see Hrouda, 1982 for the definition of the anisotropy factors referred in this text) is always well less than 1.1 (fig. 2 and table I).

Moreover, also other anisotropy factors (see table I) shows values in the range typical of nearly undeformed sediments and where careful measure of bedding attitude at the sampling site was possible it was noted (fig. 3) that the k_{min} cluster sets really close to the pole of bedding.

Where careful bedding measure at the sampling site was not possible the k_{min} cluster was compared with the trend of the bedding reported on the published geological maps and a close agreement between the obtained k_{min} axes cluster and the expected bedding pole was always observed.

The detailed analysis of the AMS from each site shows that some evidences of a sensitive influence of tectonics are present only at the sites the closest to the main structural elements (see Kligfield *et al.*, 1982 and Hrouda, 1982 for the qualitative description of the changes in shape and orientation of the susceptibility ellipsoid for a sediment progressively deformed in a directional stress field). In particular, the site LU03, close to the main strike-slip fault, is characterized by a prolate susceptibility ellipsoid with the k_{min} and k_{int} axes which tend to scatter along a girdle normal to the k_{max} cluster (fig. 4a)); also anisotropy factors show values typical of a tectonic

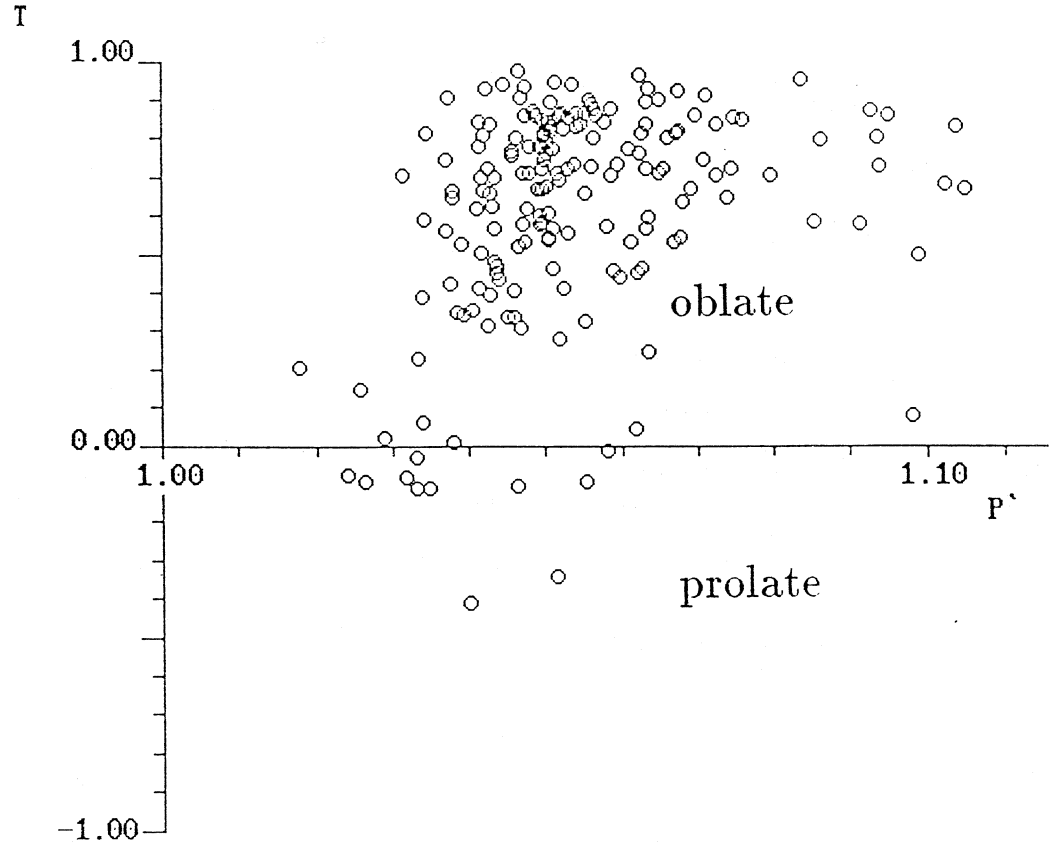

Fig. 2. Plot of T (shape factor) *versus* P' (corrected anisotropy degree) for all the analyzed specimens. T value is 0 for a neutral anisotropy ellipsoid, +1 for a uniaxial oblate ellipsoid and –1 for a uniaxial prolate ellipsoid.

fabric. A purely sedimentary (compactional) fabric, with a relatively strong magnetic foliation and the k_{max} and k_{int} axes scattered in the plane normal to the k_{min} cluster, and hence without a well-defined magnetic lineation, was found only in two sites (fig. 4b)). For all the other sites (fig. 4c)) a prevailing magnetic foliation is accompanied with a well-defined magnetic lineation with the k_{max} axes always clustered tightly close to the horizontal (nearly along the strike of the bedding).

The directional analysis of all the determined k_{max} axes reveals that such axes display a quite similar orientation (approximately NW-SE) through the whole area (fig. 5a)). The k_{max} maximum density direction for the Pleistocene sites (with an azimuth of N164°; fig. 5b)) fits very well with the expected direction of maximum extension for a compressive episode with σ_1 oriented N70°. Moreover, if we consider the two Upper Pliocene sites from the basin western edge, we observe that the k_{max} maximum density direction shows a slightly different azimuth (N131°; fig. 5c)), in agreement with the assumption that they suffered also the effects of a previous compression, with σ_1 oriented N20°.

5. Natural Remanent Magnetization (NRM) data

A pilot specimen for each site was stepwise

Table I. List of anisotropy factors computed at each site.

Sites	n	k_m	L	F	P'	T	q
LU01	18	470.8(322.4)	1.006(.004)	1.059(.012	1.072(.016)	.828(.076)	.093(.044)
			1.004	1.059	1.071	.856	.077
LU02	17	202.6(16.5)	1.006(.002)	1.035(.006)	1.045(.007)	.689(.106)	.173(.064)
			1.003	1.032	1.039	.847	.081
LU03	11	264.2(86.7)	1.020(.008)	1.029(.012)	1.051(.012)	.150(.346)	.576(.280)
			1.021	1.014	1.036	.211	.878
LU04	12	341.5(103.4)	1.003(.002)	1.039(.004)	1.047(.005)	.863(.080)	.073(.044)
			1.003	1.035	1.042	.857	.076
LU05	13	493.9(216.2)	1.004(.002)	1.053(.012)	1.064(.016)	.879(.042)	.065(.023)
			1.002	1.049	1.059	.912	.046
LU06	11	364.4(50.7)	1.003(.001)	1.045(.004)	1.054(.004)	.860(.032)	.075(.017)
			1.002	1.045	1.053	.896	.054
LU07	12	285.2(33.9)	1.007(.002)	1.036(.005)	1.047(.005)	.664(.120)	.189(.073)
			1.007	1.036	1.046	.688	.173
LU08	11	347.5(123.5)	1.010(.004)	1.052(.012)	1.066(.016)	.688(.097)	.175(.061)
			1.009	1.050	1.065	.692	.172
LU09	10	276.0(18.4)	1.009(.003)	1.037(.005)	1.050(.005)	.602(.121)	.228(.079)
			1.009	1.036	1.048	.615	.217
LU10	11	288.6(53.8)	1.014(.010)	1.054(.013)	1.073(.016)	.589(.217)	.243(.150)
			1.015	1.048	1.066	.524	.277
LU11	12	225.6(49.6)	1.013(.003)	1.021(.010)	1.034(.012)	.198(.243)	.521(.188)
			1.010	1.021	1.032	.351	.392
LU12	11	213.9(19.8)	1.014(.004)	1.046(.012)	1.064(.015)	.537(.101)	.270(.067)
			1.013	1.045	1.061	.559	.254
LU13	11	235.2(25.3)	1.005(.003)	1.037(.006)	1.046(.006)	.772(.160)	.127(.099)
			1.001	1.038	1.045	.925	.039
LU14	13	243.2(36.2)	1.012(.005)	1.029(.006)	1.043(.006)	.398(.223)	.371(.171)
			1.011	1.028	1.040	.432	.336
LU15	9	279.1(85.9)	1.015(.008)	1.028(.010)	1.045(.009)	.284(.338)	.468(.284)
			1.016	1.020	1.037	.110	.580
Total	182	307.0(155.9)	1.009(.007)	1.041(.014)	1.054(.016)	.617(.283)	.231(.201)
			1.007	1.029	1.038	.594	.230

The upper line for each locality shows the arithmetic means of the individual specimens values (standard deviation in brackets); the lower line shows the locality tensorial means (values referred in the text), determined averaging out the individual components of the specimens tensors and calculated by the ANS 21 program (Jelinek, 1978).

n = number of samples;

$k_m = (k_{max} + k_{int} + k_{min}) / 3$ (mean susceptibility, in 10^{-6} SI units);

$L = k_{max} / k_{int}$ (lineation);

$F = k_{int} / k_{min}$ (foliation);

$P' = \exp\sqrt{2\left[(\eta_1 - \eta)^2 + (\eta_2 - \eta)^2 + (\eta_3 - \eta)^2\right]}$ (corrected anisotropy degree);

$T = 2(\eta_2 - \eta_3) / (\eta_1 - \eta_3) - 1$ (shape factor);

$q = \dfrac{(k_{max} - k_{int})}{\left[(k_{max} + k_{int})/2 - k_{min}\right]}$ (shape factor);

$\eta_1 = \ln k_{max}$, $\eta_2 = \ln k_{int}$, $\eta_3 = \ln k_{min}$, $\eta = (\eta_1 + \eta_2 + \eta_3) / 3$.

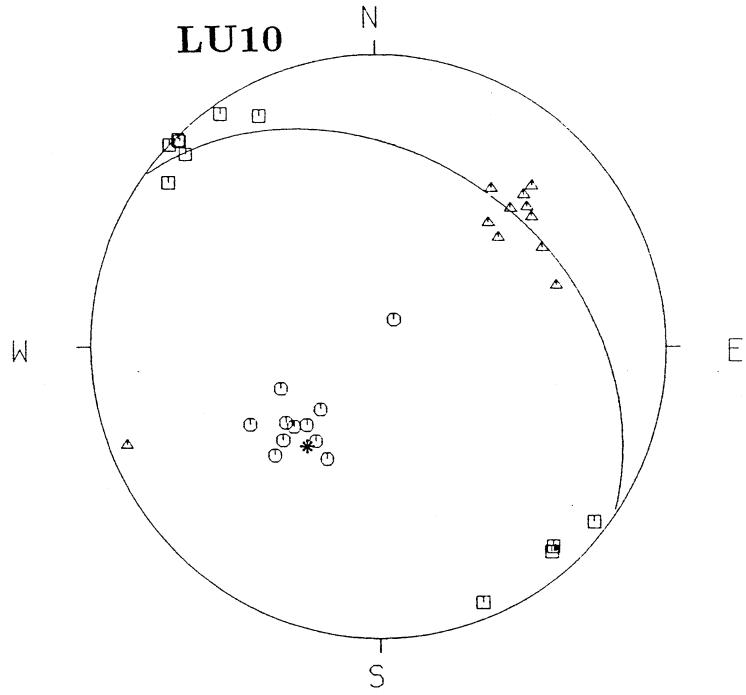

Fig. 3. Orientations of the principal susceptibility axes for specimens from site LU10. □ k_{max}; △ k_{int}; ○ k_{min}. The bedding plane and its pole (*) are also drawn. Schmidt equal-area projection, lower emisphere.

thermally demagnetized. At each heating step the magnetic susceptibility of each pilot was measured. Significant increases in the susceptibility values were observed in the range (310÷340)°C (fig. 6).

Such increases in susceptibility were also associated with drastic changes in the magnitude and direction of the residual magnetization. Thermal demagnetization of the pilots was stopped at 400°C (10^{th} step).

On the basis of the pilot's behaviour the remaining specimens (one for each core) were demagnetized in 7-9 steps, always monitoring the variations in their magnetic susceptibility, up to (340÷360)°C, at which point their magnetic properties had already undergone a major change. The initial NRM intensities were generally of order of 10^{-3} A/m, rainging from 1.1×10^{-4} A/m to 1.3×10^{-1} A/m and at the temperatures corresponding to the main magnetic changes the intensity of the residual NRM reached the (10÷20)% of the initial value for most of the specimens.

For each site specimens with a single stable component of magnetization (giving stable endpoints onto spherical projection and lines toward the origin in a Zijderveld diagram; fig. 7a)) as well as with two components with stability spectra partly overlapping (giving «remagnetization» circles on a stereonet; fig. 7b)) were recognized. Best-fit lines and planes were evaluated by means of the principal components analysis, according to the method developed br Kirschvink (1980). Paleomagnetic directions for each site were calculated by the combined analysis of stable endpoints and remagnetization circles (McFadden and McElhinny, 1988) (fig. 7c)).

Paleomagnetic data were considered both before and after bedding correction. The mean paleomagnetic directions for each site are listed in

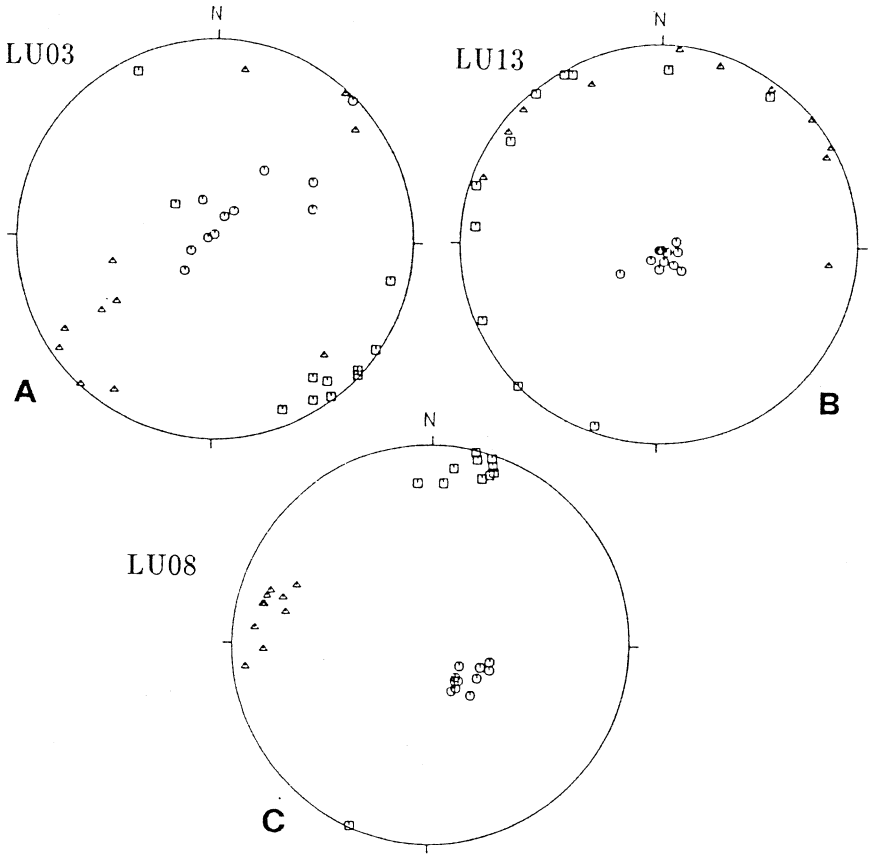

Fig. 4. Orientations of the principal susceptibility axes for specimens from sites LU03, LU13 and LU08, before bedding correction. Symbols as in fig. 3. A) Tectonic fabric – k_{int} and k_{min} directions tend to scatter along a girdle normal to the k_{max} cluster (close to the horizontal); B) purely sedimentary fabric – only the magnetic foliation is well developed; the k_{max} and k_{int} axes are dispersed in the plane normal to the k_{min} cluster; C) «mixed» fabric – each of the k-axis is grouped in a well-defined cluster. Schmidt equal-area projection, lower emisphere.

table II and plotted onto an equal-area projection in fig. 8.

The overall mean was calculated using Fischer's (1953) statistics. The sites LU11 and LU12 were discarded for their structural position (at the overthrust front). Bedding correction produces a significant decrease of scattering; the fold tests (both the McElhinny (1964) and the McFadden and Jones (1981) tests) are positive at the 95% of confidence. The only site with a normal paleomagnetic direction (LU10) is antipodal to the cluster of the reversed sites, after bedding correction.

6. Conclusions

The results obtained from the AMS analysis of the Plio-Pleistocene clayey units of the Sant'Arcangelo basin indicate in summary that:

– the magnetic foliation is close to the bedding plane;
– the magnetic lineation is perpendicular to the shortening direction.

Such results are quite similar to those obtained from apparently undeformed clays coming from

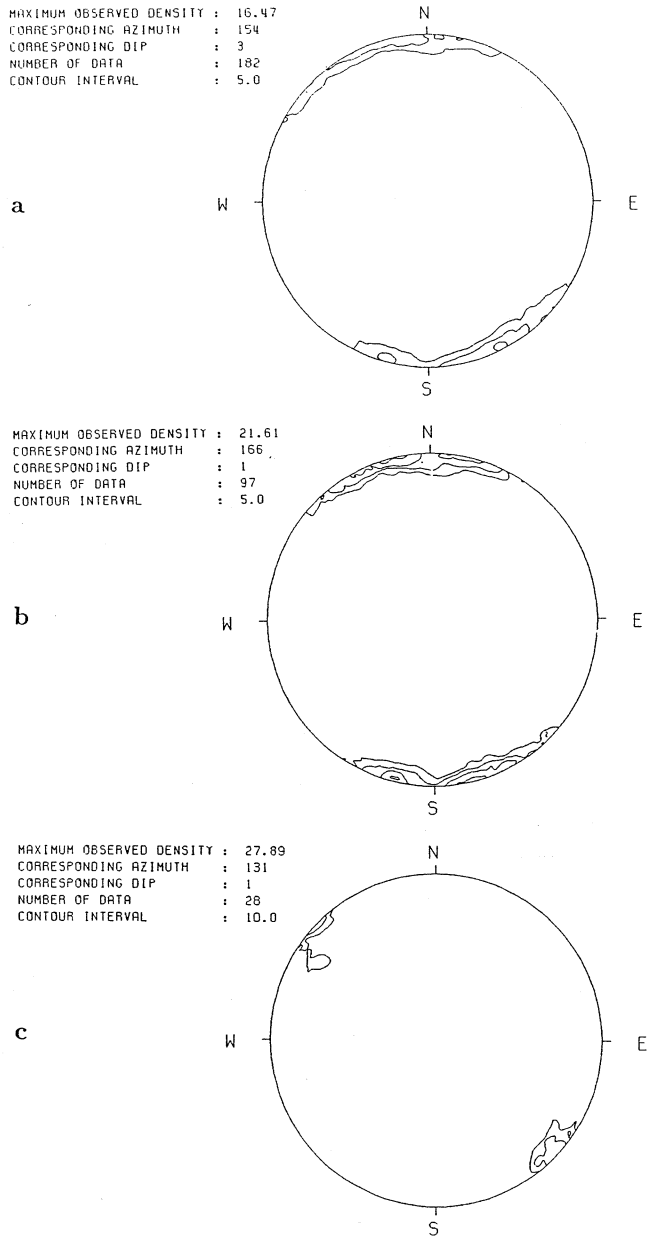

Fig. 5. Contour plots of the magnetic lineations (k_{max} axes), after bedding correction, obtained for: a) all specimens; b) specimens from Upper Pliocene-Lower Pleistocene sites in the eastern flank of the main syncline of the basin (except LU04 and LU13 which show no magnetic lineation); c) specimens from Upper Pliocene sites of the western flank of the main syncline of the basin. «Density» refers to the percentage number of data points per 1% of the plotting area. Schmidt equal-area projection, lower emisphere.

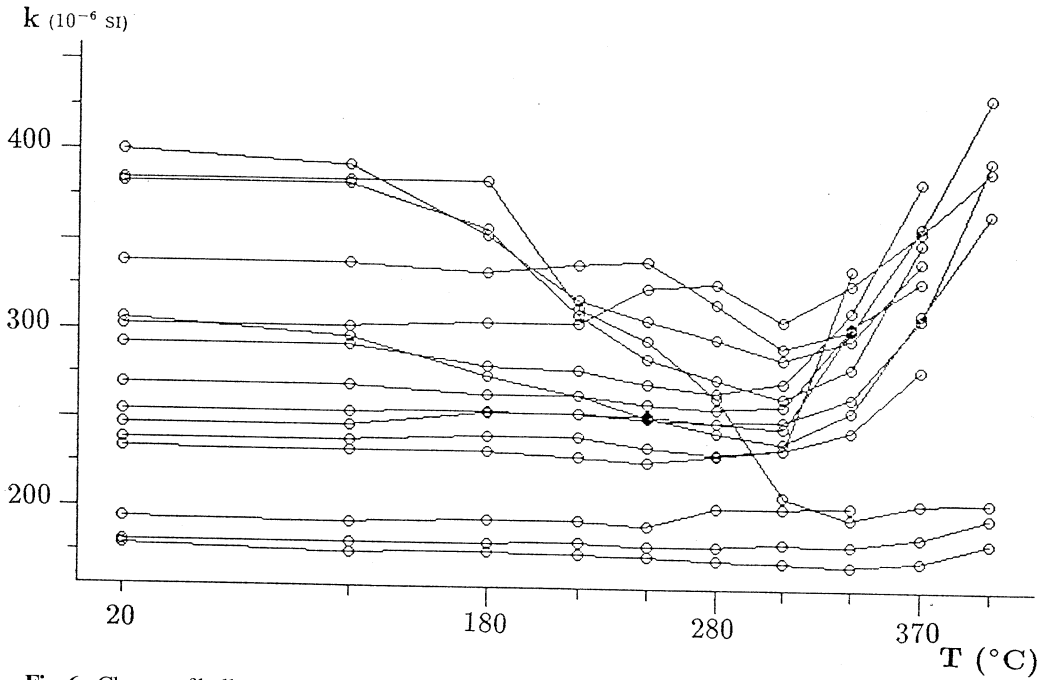

Fig. 6. Change of bulk magnetic susceptibility during step heating (pilots). Each line represents one specimen.

other regions of the world with evidence of large-scale compressional events (Kissel *et al.*, 1986). Results indicate that the clayey units here studied are characterized by a magnetic fabric typical of sediments at the very first stage of deformation. On this basis, the AMS results allow the determination of the bedding attitude (that is, the structural setting) for each sampling site, even where the clays seem quite homogeneous or where is however difficult to take a careful measure of the local bedding attitude in the field.

At the same time, the results obtained indicate that the orientations of the k_{max} axes are strictly associated with the direction of the compressive stresses to which the sampled units were subjected and also that the shape of the susceptibility ellipsoids is related to the structural position of the sampling site. The above observations suggest that the AMS data allow the reconstruction of the strain pattern in the basin, that is, the estimate, for each sampling site, of the relative degree of strain and of the local direction of the principal strain axes.

The study of the NRM of the Plio-Pleistocene clayey units of the Sant'Arcangelo basin has given results which can be summarized as follows:

– The paleomagnetic vectors obtained from the analysis of the demagnetization paths of the specimens from each site are a statistic estimate of a primary component of magnetization, as indicated by positive fold tests and antipodality between normal (LU02) and reversed (all other sites) site mean directions. So we expect that the overall mean direction reflects the local geomagnetic vector at the time of deposition (for Upper Pliocene-Lower Pleistocene it ought to be $D \simeq 180°$, $I \simeq -56°$ for a reverse geomagnetic field).

– The mean direction obtained from the statistical analysis of 13 sampled sites (after bedding correction) is $D = 157.8°$, $I = -56.1°$ ($\alpha_{95} = 3.7°$), indicating a counterclockwise rotation of about 22° of the Sant'Arcangelo basin. Flattening of the paleomagnetic vectors is absent or negligible.

– No significant difference has been detected for Pliocene and Pleistocene sites, suggesting that counterclockwise rotation we observe occurred after the deposition of the Lower Pleistocene clays.

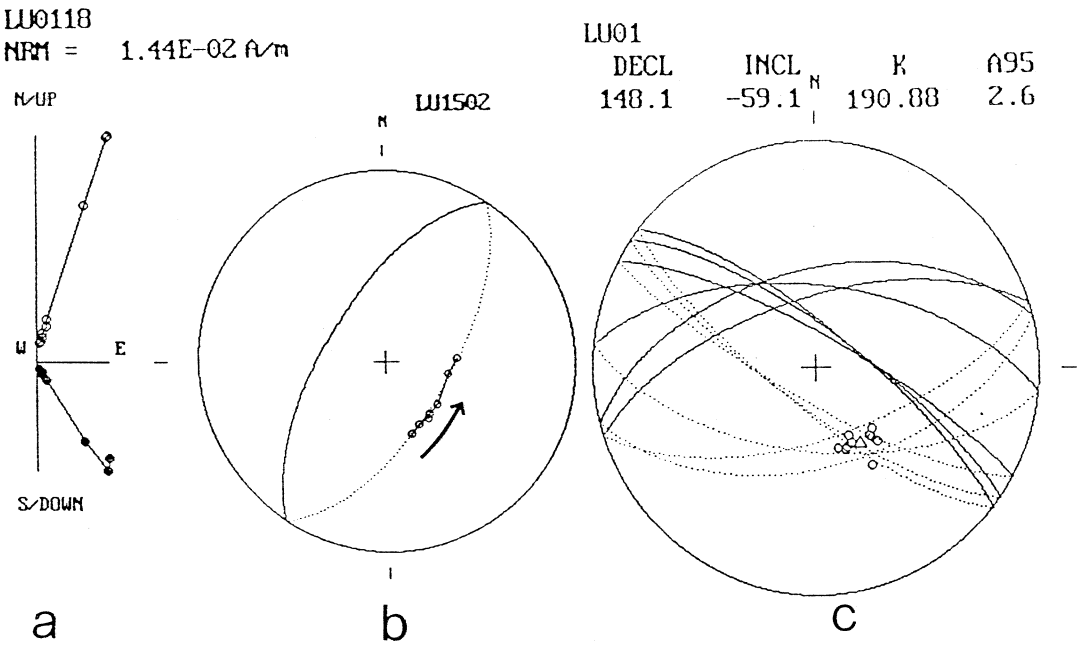

Fig. 7. a) Representative vector diagram of a specimen (LU0118) with a single stable component of magnetization. Full circles – horizontal projection; open circles – vertical projection. b) Representative demagnetization path for a specimen (LU1502) which defines a remagnetization circle. Solid line – lower hemisphere; open circles and dotted line – upper hemisphere. c) Example of convergence for remagnetization circles and stable endpoints for a site (LU01). Open triangle – convergence point.

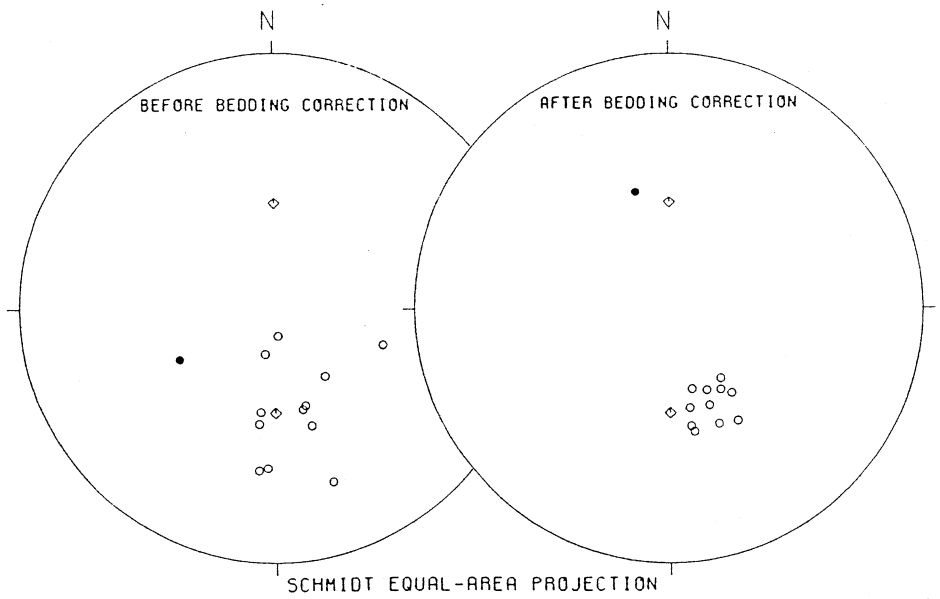

Fig. 8 Stereonets with the site mean directions listed in table II. Full circles – normal magnetization; open circles – reversed magnetization; ◇ present and reversed (antipodal) directions of the geomagnetic field.

Table II. Mean paleomagnetic directions computed at each site from combined analysis of remagnetization circles and stable endpoints.

		Before bedding correction				After bedding correction			
Sites	$N(n,c)$	D	I	K	α_{95}	D	I	K	α_{95}
LU01	17(11,6)	163.2	–57.5	190.9	2.6	148.1	–59.1	190.9	2.6
LU02	14(11,3)	242.0	55.3	11.1	12.5	344.1	51.1	26.9	7.9
LU03	10(0,10)	163.3	–50.5	30.1	9.9	158.0	–56.3	30.1	9.9
LU04	9(5,4)	165.9	–56.5	304.5	3.1	148.7	–59.1	304.5	3.1
LU05	10(5,5)	188.0	–56.6	39.4	8.0	156.5	–61.9	39.4	8.0
LU06	9(6,3)	188.5	–52.6	40.6	8.4	169.8	–57.2	40.6	8.4
LU07	11(4,7)	192.3	–75.4	210.7	3.3	165.5	–63.7	210.7	3.3
LU08	11(3,8)	174.1	–81.8	157.9	3.8	144.7	–62.3	157.9	3.8
LU09	10(6,4)	183.2	–37.3	27.0	9.7	169.5	–49.7	27.0	9.7
LU10	8(5,3)	109.3	–53.4	93.7	5.9	157.4	–49.6	93.7	5.9
LU11(*)	10(1,9)	136.7	–46.6	18.0	12.6	195.2	–60.9	18.0	12.6
LU12(*)	8(2,6)	142.8	–24.8	28.7	11.4	133.5	–27.2	28.7	11.4
LU13	11(7,4)	144.7	–63.2	117.3	4.3	144.4	–56.2	117.3	4.3
LU14	9(2,7)	162.0	–29.0	18.3	13.2	149.4	–47.8	18.3	13.2
LU15	6(1,5)	186.6	–36.1	27.4	15.4	170.8	–51.0	27.4	15.4
Mean:	13	168.3	–56.1	17.8	9.2	157.8	–56.1	111.2	3.7

(*) Sites rejected for their structural position (see text). The overall mean is computed using Fisher's statistics; for site LU02 the antipodal (reversed) direction was considered. N: number of samples (n = number of direct observations; c = number of remagnetization circles); D, I: declination and inclination; K: precision parameter; α_{95}: half-angle of cone of 95% confidence about the mean direction.

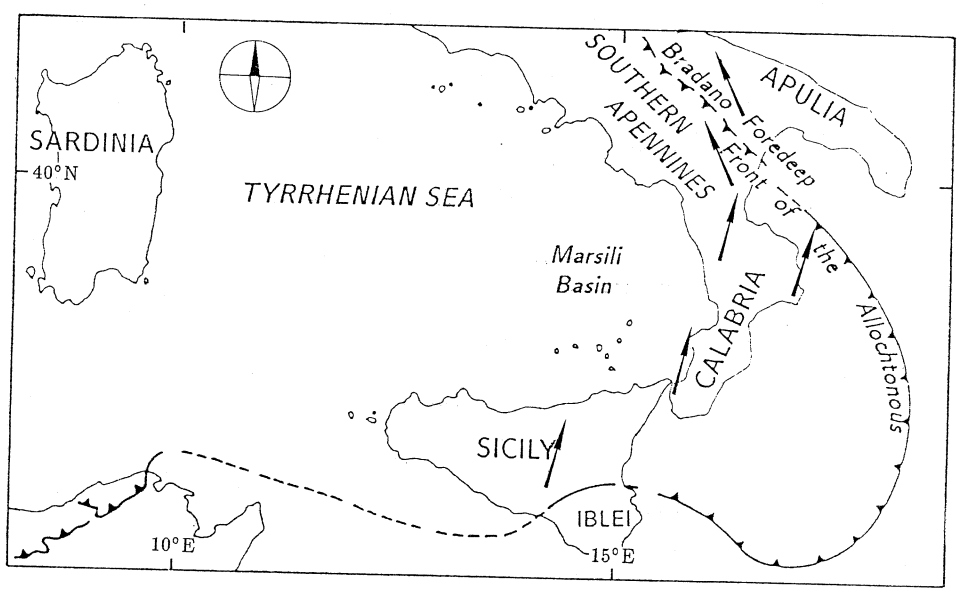

Fig. 9. Paleomagnetic declinations (arrows) reported in the literature for Pleistocene sediments in southern Italy (the sketch is only indicative and locations of arrow origin are approximate). Data from Tauxe *et al.*, 1983; Aifa *et al.*, 1988; Scheepers *et al.*, 1991; Sagnotti, 1992.

This estimate is apparently surprising if we consider that a similar amount of vertical-axis rotation, with respect to the African pole, was recognized for some different structural domains in the Italian peninsula since the Mesozoic (see Lowrie, 1986 for a review); however, recently reported paleomagnetic data from other areas in southern Italy indicate that such relatively high amount of vertical-axis rotation is a common feature for the Pleistocene units (fig. 9).

These data describe a pattern of Pleistocene rotations which seems to be of regional significance and indicate that: 1) the Bradano foredeep (Matera area) experienced a counterclockwise rotation quite similar to the one here found for the Sant'Arcangelo basin (Scheepers *et al.*, 1991); 2) there is a uniform clockwise rotation of 15° widely recognized both in Calabria and in Sicily (excluding Iblei foreland) (Tauxe *et al.*, 1983; Aifa *et al.*, 1988; Scheepers *et al.*, 1991).

In our opinion southeastward migration of rifting and spreading processes in the Tyrrhenian Sea (the basaltic crust formation in the Marsili basin occurred in the last 1.9 million years, during which the basin opened at a full spreading rate of 3.5 cm/y and subsided at a rate of 700 m/My; Kastens *et al.*, 1988) may be associated with the observed pattern of Pleistocene rotations. Opening in the Marsili area, indeed, fits well with the measured counterclockwise rotation in southern Apennines and clockwise rotation in Calabria and Sicily, resulting in a Pleistocene increase in the peri-Tyrrhenian belt curvature.

Acknowledgments

We wish to thank Prof. E. Boschi, Prof. R. Funiciello and Dr. C. Lay for their encouragement and useful suggestions.

REFERENCES

AIFA, T., H. FEINBERG and J.P. POZZI (1988): Pliocene-Pleistocene evolution of the Tyrrhenian arc: paleomagnetic determination of uplift and rotational deformation, *Earth Planet. Sci. Lett.*, **87**, 438-452.

CALDARA, M., F. LOIACONO, E. MORLOTTI, P. PIERI and L. SABATO (1988): Caratteri geologici e paleoambientali dei depositi plio-pleistocenici del bacino di S. Arcangelo (parte settentrionale): Italia meridionale, *Atti 74° Congr. Soc. Geol. Ital.*, **B**, pp. 51-58.

FISHER, R.A. (1953): Dispersion on a sphere, *Proc. R. Soc. London, Ser. A*, **217**, 295-305.

HIPPOLYTE, J.C., J. ANGELIER, F. ROURE and C. MULLER (1991): Géometrie et mécanisme de formation d'un bassin «piggyback»: le bassin de Sant'Arcangelo (Italie méridionale), *C. R. Acad. Sci. Paris*, **312**, Série II, 1373-1378.

HROUDA, F. (1982): Magnetic anisotropy of rocks and its application in geology and geophysics, *Geophys. Surv.*, **5**, 37-82.

JELINEK, V. (1978): Statistical processing of anisotropy of magnetic susceptibility measured on groups of specimens, *Stud. Geophys. Geod.*, **22**, 50-62.

INCORONATO, A. and G. NARDI (1989): Paleomagnetic evidences for a peri-Tyrrhenian orocline, in «The Lithosphere in Italy», edited by A. BORIANI *et al.*, *Atti Conv. Acc. Naz. dei Lincei*, **80**, 217-227.

KASTENS, K.A. *et al.* (1988): ODP Leg 107 in the Tyrrhenian Sea: insights into passive margin and back-arc basin evolution, *Geol. Soc. Am. Bull.*, **100**, 1140-1156.

KIRSCHVINK, J.L. (1980): The least-square line and plane and the analysis of paleomagnetic data, *Geophys. J. R. Astron. Soc.*, **62**, 699-718.

KISSEL, C., E. BARRIER, C. LAY and T.Q. LEE (1986): Magnetic fabric in «undeformed» marine clays from compressional zones, *Tectonics*, **5**, 769-781.

KLIGFIELD, R., W.H. OWENS and W. LOWRIE (1982): Magnetic susceptibility anisotropy, strain and progressive deformation in Permian sediments from the Maritime Alps (France), *Earth Planet. Sci. Lett.*, **55**, 181-189.

LENTINI, F. (1979): Le unità sicilidi della Val d'Agri (Appennino Lucano), *Geologica Rom.*, **18**, 215-224.

LOWRIE, W. (1986): Paleomagnetism and the Adriatic promontory: a reappraisal, *Tectonics*, **5**, 797-807.

MCELHINNY, M.W. (1964): Statistical significance of the fold test in paleomagnetism, *Geophys. J. R. Astron. Soc.*, **8**, 338-340.

MCFADDEN, P.L. and D.L. JONES (1981): The fold test in paleomagnetism, *Geophys. J. R. Astron. Soc.*, **67**, 53-58.

MCFADDEN, P.L. and M.W. MCELHINNY (1988): The combined analysis of remagnetization circles and direct observations in paleomagnetism, *Earth Planet. Sci. Lett.*, **87**, 161-172.

PATACCA, E. and P. SCANDONE (1989): Post-Tortonian mountain building in the Apennines. The role of the passive sinking of a relic lithospheric slab, in «The Lithosphere in Italy», edited by A. BORIANI *et al.*, *Atti Conv. Acc. Naz. dei Lincei*, **80**, 157-176.

PATACCA, E., R. SARTORI and P. SCANDONE (1990): Tyrrhenian basin and Apenninic arcs: kinematic relations since late Tortonian times, *Mem. Soc. Geol. Ital.* (in press).

SAGNOTTI, L. (1992): Paleomagnetic evidence for a Pleistocene counterclockwise rotation of the Sant'Arcangelo basin, *Geophys. Res. Lett.*, **19**, 135-138.

SAGNOTTI, L. and F. SPERANZA (1992): Magnetic fabric analysis of the Plio-Pleistocene clayey units of the Sant'Arcangelo basin, Southern Italy, submitted to *Phys. Earth Planet. Inter.*

SCHEEPERS, P.J.J., C.G. LANGEREIS and J.D.A. ZIJDERVELD (1991): Differential tectonic rotations along the Tyrrhenian arc, *IAGA Abstract XX General Assembly IUGG: 87, Vienna, August 11-24, 1991.*

TAUXE, L., N.D. OPDYKE, G. PASINI and C. ELMI (1983): Age of the Plio-Pleistocene boundary in the Vrica section, southern Italy, *Nature*, **304**, 125-129.

VEZZANI, L. (1967): Il bacino plio-pleistocenico di S. Arcangelo (Lucania), *Atti Acc. Gioenia Sc. Nat.* (Suppl. Sc. Geol.) s. VI, **18**, 207-227.